

A Social-Welfare based OPF for Integrated Power System with Unified Power Flow Controller

Md.Yaseen¹, Sravana Kumar Bali^{2*}

¹Research Scholar, Department of EEE, GITAM Deemed to be University, Visakhapatnam, Andhra Pradesh, India. yaseen.eee08@gmail.com

²Assistant Professor, Department of EEE, GITAM Deemed to be University, Visakhapatnam, Andhra Pradesh, India. sravanbali@gmail.com

Abstract: In the present transmission systems, it has become mandatory to utilize the available resources and also to substitute it with the renewable energy sources at the earliest. The optimal utilization of the resources provides an added advantage of reduction of its cost to the end consumers of electrical energy. In this paper, a multi-objective optimal power flow (OPF) in the existence of FACTS devices has been proposed for an integrated transmission system. The uniqueness of this paper is the choice of the multi-objective function. The objective function includes minimization of voltage deviation, power loss and negative social welfare (NSW). The reduction of loss and NSW ensures the reduction of per-unit charge of electricity at the customer-end leading to a greater customer satisfaction. The FACTS device used for the problem is Unified Power Flow Controller (UPFC). The hypothesis has been applied on an IEEE 30 bus system. The Mouth Flame Optimization Algorithm has been used for the optimization of objective function. The results obtained have been presented, compared and analysed in detail.

1. INTRODUCTION

India is an overpopulated nation with growing power demand. The deregulation of the power industry has further increased the pressure on the transmission corridors in the country. Consequently, optimization of power flow has gained immense importance in the power world. At the same time, the use of FACTS devices in the AC transmission system is the only cost-effective solution to match the high efficiency of the HVDC systems.

M.O.Lawal et.al [1] suggested a technique for handling the congestion constraints in an optimal power flow process for hydro-thermal system. A power flow tracing strategy is used to locate generators that lead to line congestion and penalize them by increasing their outputs to accomplish this remedy. The congestion is then eliminated by setting a penalized value for the maximum power of the generators affected. I.Batra et.al [2] explained the implementation of the TECM-PSO algorithm (TECM) to the non-linear congestion management problem of a deregulated power system for the advanced twin extremity mapping of the chaotic map. K. Teeparthi et.al [3] implemented the hybrid PSO-APO algorithm considering the wind and thermal generators for contingency conditions.

Power system problems have been successfully resolved with FACTS devices [4]. A method to install a Unified Power Flow Controller (UPFC) at the proper position while taking contingencies was proposed by Visakha et al. in [5]. In the presence of TCSC, The optimal power flow of a power system with renewable systems has been performed by Nusair et al. [6]. Authors have used OPF when surrounded by FACTS devices to cut expenditures [7]. In the presence of TCSC and UPFC, the authors have performed OPF for an integrated wind farm system to reduce expenses [8]. FACTS device deployment and tuning must be done properly in order to address the various power system problems. Power system congestion and contingency issues have been successfully resolved with IPFC [9,10]. Since an IPFC has multiple terminals, it is necessary to plan the ideal position for each IPFC converter [11]. A voltage index-based contingency analysis has been proposed in [12]. For the purpose of enhancing voltage stability, Kumar et al. [13] have suggested a cat swarm optimization-based approach of IPFC placement. For voltage stability, Verma et al. [14] suggested placing FACTS devices in the ideal location. Control of FACTS devices has been studied in the context of

integrated power systems [15, 16]. In addition to technical concerns like voltage improvement, the positioning and sizing of FACTS devices for the highest social welfare, lowering the cost of load shedding and building new branches has been suggested in [17]. It has been noted that increasing social welfare is a matter that is more in line with the application of optimization. For a multi objective function, [18, 19] developed and successfully tested a combination of optimal power flow and placement and sizing of FACTS.

The conventional OPF focuses solely on the prices charged by suppliers. The idea of consumer advantage must be included into the market model so that consumers can be considered. A product's consumer benefit is the value it adds to the user's life. Consumer gain can be expressed mathematically as a function of demand. For the provider, it's like cost, but with a minus sign. Social welfare can be calculated by subtracting the total consumer benefits from the total supplier expenses once consumer benefit has been specified.

In this paper, a multi-objective OPF for an integrated power system has been proposed. The transmission network consists of the conventional generators, solar and a wind power unit. The objective of optimization is the minimization of losses voltage deviation and improvement of social welfare. Since, it is a minimization function; a negative social welfare has been developed to fit the objective function. The objectives have been achieved in three steps. Firstly, an OPF of the integrated system has been performed for the multi-objective function. An index based optimal position for the placement of UPFC has been then sorted in the power system. The UPFC has been optimally tuned for further achieving the objectives. Finally, the integrated system has been once again optimized for the realization of the objectives of testing the system for its durability, contingency analysis has been performed on the system. The results have been presented and analyzed which emphasizes on the robustness of the system under unstable operating conditions. An IEEE 30 bus system has been used for the study. The Moth Flame optimization algorithm and an IEEE 30 bus system have been used for the study.

2. MULTI OBJECTIVE PROBLEM FORMULATION

The work consists of minimization of the multi-objective function which consists of the following objectives

Objective 1: Negative Social Welfare

In order to maximise social welfare, one must raise the demand side cost, also known as the seller side cost, while lowering the generating side cost. Social welfare is defined as the difference between the overall benefits of buyers and sellers. Since it is a minimization function, hence a negative of the social welfare is minimized.

$$NSW = \sum_{i=1}^{NG} C_i(P_{Gi}) - \sum_{j=1}^{ND} B_j(P_{Dj}) \tag{1}$$

$$C(P_g) = \sum_{i=1}^n a_{gi} P_{gi}^2 + b_{gi} P_{gi} + c_{gi} \tag{2}$$

$$B(P_d) = \sum_{i=1}^n a_{di} P_{di}^2 + b_{di} P_{di} + c_{di} \tag{3}$$

Where,

$C(P_g)$ = Cost of generation

P_{Gi} = Power generation at bus i

a_{gi}, b_{gi}, c_{gi} = generator cost coefficients

$B(P_d)$ = Demand side bidding

a_{di}, b_{di}, c_{di} = Load cost coefficients

P_{di} Real Power demand at bus i

Objective 2: Minimization of Power Loss

$$F_2 = \sum_{k=1}^{NT} G_{k(i,j)} [V_i^2 + V_j^2 - 2V_i V_j \cos(\delta_{ij})] \quad (4)$$

Where,

V_i, V_j = Voltage at bus i, j in p.u.

Objective 3: Voltage deviation minimization

The voltages must be correctly maintained in order to lessen the voltage collapse in order to obtain a decent voltage profile and reduce the large voltage swells. The following is the objective function for reducing voltage deviation:

$$F_3 = \sum_{i=1}^{N_B} \| V_m - 1 \| \quad (5)$$

The voltage at the bus m and the number of buses are both represented by V_m and N_B

Constraints-

$$\sum_{i=1}^{NG} P_{Gi} - P_{Loss} - P_L = 0 \quad (6)$$

$$P_{Loss} = \sum_{j=1}^{N_{TL}} G_j [|V_i|^2 + |V_j|^2 - 2|V_i||V_j|\cos(\delta_i - \delta_j)] \quad (7)$$

$$P_i - \sum_{k=1}^{N_b} |V_i V_k Y_{ik}| \cos(\theta_{ik} - \delta_i + \delta_k) = 0 \quad (8)$$

$$Q_i - \sum_{k=1}^{N_b} |V_i V_k Y_{ik}| \sin(\theta_{ik} - \delta_i + \delta_k) = 0 \quad (9)$$

Inequality Constraints

$$V_i^{\min} \leq V_i \leq V_i^{\max}$$

$$\phi_i^{\min} \leq \phi_i \leq \phi_i^{\max}$$

$$TL_1 \leq TL_1^{\max}$$

$$P_{Gi}^{\min} \leq P_{Gi} \leq P_{Gi}^{\max}$$

$$Q_{Gi}^{\min} \leq Q_{Gi} \leq Q_{Gi}^{\max}$$

$$V_{vr}^{\min} \leq V_{vr} \leq V_{vr}^{\max}$$

$$\delta_{vr}^{\min} \leq \delta_{vr} \leq \delta_{vr}^{\max}$$

$$V_{cr}^{\min} \leq V_{cr} \leq V_{cr}^{\max}$$

$$\delta_{cr}^{\min} \leq \delta_{cr} \leq \delta_{cr}^{\max}$$

V_{vr} is the shunt converter voltage magnitude (p.u), δ_{vr} is the shunt converter phase angle, V_{cr} is the series converter voltage magnitude (p.u), δ_{cr} is the series converter phase angle.

3. PROPOSED METHODOLOGY

The multi-objective OPF problem is solved in the following step by step procedure-

1. The solar and wind power units are placed at chosen buses in the transmission system.
2. The OPF is conducted for the multi objective function.
3. The location for the placement of UPFC is calculated using L-index. The L-index measures the actual state of stability of the system with respect to its stability limit. It measures the stability of the complete system:

$$L = \max_{j \in \alpha_L} \{L_j\} = \max_{j \in \alpha_L} \left| 1 - \frac{\sum E_{ji} V_i}{V_j} \right| \tag{16}$$

Where α_L , α_G are the load and generator buses respectively. The L index varies in the range between 0 to 1. $L = 0$ at no load while it is 1 at a point near voltage collapse.

4. The OPF and optimal tuning of the UPFC is performed for the multi objective function.
5. The robustness of the system is tested by performing contingency analysis of the above system.

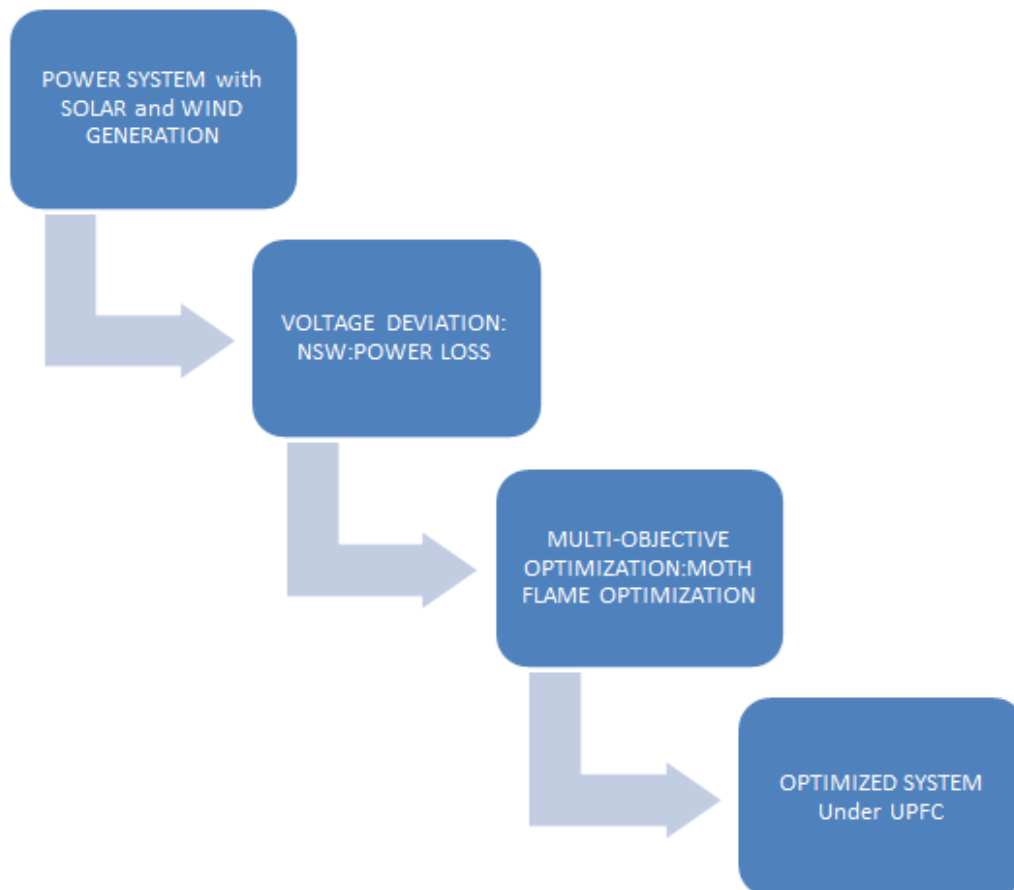


Figure 1: Block diagram of proposed methodology

4. MOTH FLAME OPTIMIZATION

It is an optimization concept inspired by nature. The moths' nighttime navigation strategy served as inspiration for the algorithm. The moths move at a constant inclination to the moon. The moths also have a propensity to circle the lights in a spiral motion. It is presumed that the moths symbolize the multi-objective function's solution. The moths' location in the space is one of the problem's variables. The mathematical modelling of the Moths' behavior is as mentioned below:

Where S is the spiral function, M_i is the i -th moth, F_j denotes the j -th flame, and In light of these considerations, we define the MFO algorithm's logarithmic spiral as follows:

$$M_i = S(M_i, F_j) \tag{10}$$

$$S(M_i, F_j) = D_i \cdot e^{bt} \cdot \cos(2\pi t) + F_j \tag{11}$$

Where D_i denotes the separation between the i -th moth and the j -th flame, b is a constant used to specify how the logarithmic spiral will look, and t is a random value between the range $[-1, 1]$ and is given by:

$$D_i = |F_j - M_i| \tag{12}$$

Where M_i is the i th moth for the j th flame and D_i is the distance between them.

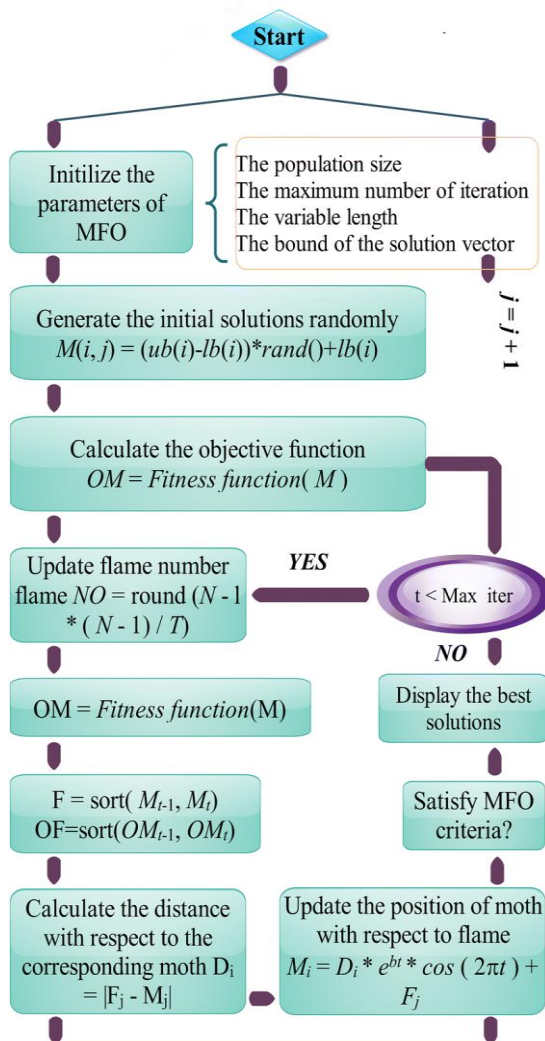


Figure 2: Flow Chart of Moth Flame Algorithm

5. RESULTS AND DISCUSSION

An IEEE 30 bus system with 41 transmission lines, 5 PV buses, one slack bus and remaining load buses have been shown in Fig. 1. Only load buses have been considered for UPFC placement. The last two thermal generators at bus 23 and 27 are replaced with solar and wind generators respectively. The generator reallocation for IEEE-30 bus system is studied. The OPF is performed for single objective functions followed by the multi-objective function optimization and the results have been compared in Table 1. OF1 represents the objective Negative Social welfare, OF2 represents Voltage Deviation, OF3 represents active power loss and OF4 represents Multi-objective Optimization. It is observed OF1 achieves the minimum value of NSW, OF2 achieves minimum voltage deviation 1.2 p.u. OF3 attains minimum active power loss of 4.24 MW, while with the multi-objective function reasonably optimum values of all the four objectives have been achieved. Equal priority has been given to each of the objectives in this study, but the weightage can be changed as per requirement.

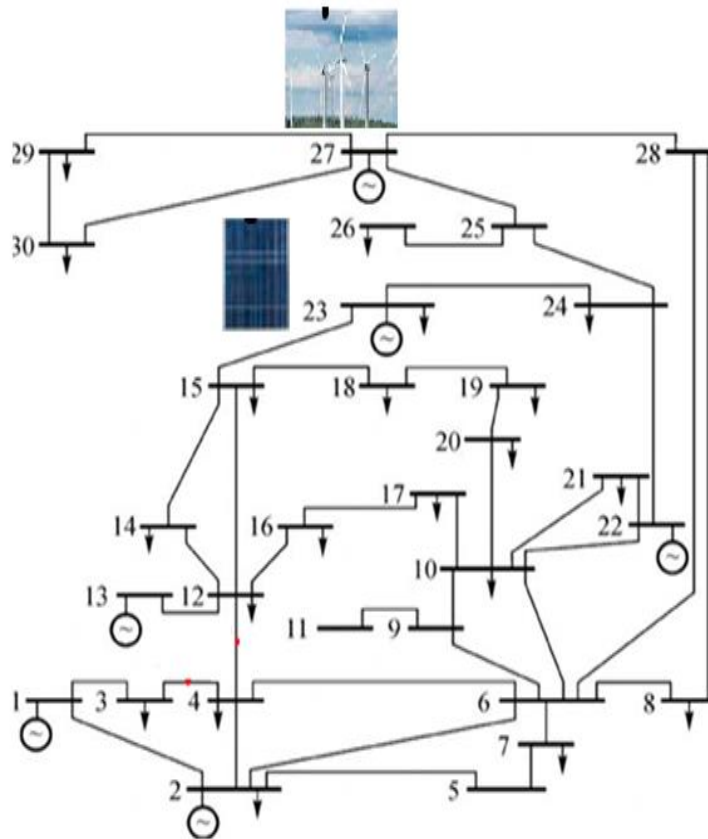


Figure 3 Modified IEEE 30 Bus Transmission System

Table-1 Generation reallocation using MFO algorithm without UPFC on IEEE 30 bus system

S.No	Parameter	OF ₁	OF ₂	OF ₃	OF ₄	
1	Real power generation (MW)	P _{G1}	153.7853	50.0000	50.0000	54.1313
		P _{G2}	43.9717	80.0000	80.0000	58.3613
		P _{G5}	20.3108	50.0000	50.0000	50.0000
		P _{G8}	10.0000	60.0000	42.6456	60.0000
		P _{Gs}	35.0000	35.0000	35.0000	35.0000
		P _{Gw}	30.0000	30.0000	30.0000	30.0000
2	Total Active power generation (MW)	293.0678	305	287.6456	287.4926	
3	Total real power generation cost (Rs/hr)	586.4685	792.5050	721.3178	712.1188	

S.No	Parameter	OF ₁	OF ₂	OF ₃	OF ₄
4	Active power Loss (MW)	9.6678	21.6000	4.09	4.24
5	Valve point effect(Rs/hr)	613.6008	835.3258	763.6632	761.4361
6	Voltage deviation (p.u.)	2.2036	1.2071	1.2753	1.2127
7	Carbon Emission(ton/hr)	0.1283	0.0595	0.0509	0.0491
8	FPL	49.4666	49.4666	49.4666	49.4666
9	FPG	586.4685	792.5050	721.3178	712.1188
10	NSW	537.0019	743.0384	671.8512	662.6522
11	Objective function	537.0019	1.2071	4.2456	1.1932e+03

Table-2 Severity Index values for all BUSES of IEEE 30 bus system

RANK	BUS NUMBER	LJ
1	30	0.0816
2	26	0.0785
3	9	0.0741
4	29	0.0673
5	24	0.0612
6	19	0.0593
7	18	0.0586
8	25	0.0567
9	23	0.0532
10	20	0.0531
11	21	0.0519
12	15	0.0509
13	14	0.0489
14	22	0.0437
15	27	0.0434

Table-3 Generation reallocation using MFO algorithm with UPFC at bus 30 on IEEE 30 bus system

S.No	Parameters	OF ₁	OF ₂	OF ₃	OF ₄
1	P _{G1}	153.0473	75.3153	56.9351	73.0849
	P _{G2}	43.3022	80.0000	80.0000	64.0341
	P _{G5}	19.6081	50.0000	50.0000	50.0000
	P _{G8}	10.0000	35.0000	35.0000	35.0000
	P _{Gs}	35.0000	35.0000	35.0000	35.0000
	P _{Gw}	30.0000	12.0000	30.0000	30.0000
2	Total Active power generation (MW)	290.9576	287.3153	286.9351	287.119
3	Total real power generation cost (Rs/hr)	579.4931	754.0696	708.1938	680.1837
4	Active power Loss (MW)	7.5575	3.9153	3.5351	3.7190
5	Valve point effect(Rs/hr)	605.6101	808.4632	752.6550	737.4227

S.No	Parameters	OF ₁	OF ₂	OF ₃	OF ₄	
6	Voltage deviation (p.u.)	0.3185	0.3046	0.3128	0.3132	
7	Carbon Emission(ton/hr)	0.1268	0.0642	0.0518	0.0528	
8	PQ send	0.0882	0.0879	0.0885	0.0884	
9	PQ rec	0.0834	0.0839	0.0844	0.0843	
10	Size	Vcr	0.0350	0.0350	0.0350	0.0350
		Tcr	-87.1236	-87.1236	-87.1236	-87.1236
		Vvr	1.0061	1.0060	1.0062	1.0062
		Tvr	-13.7096	-11.4163	-10.3741	-10.7152
11	FPL	49.4666	49.4666	49.4666	49.4666	
12	FPG	579.4931	754.0696	708.1938	680.1837	
13	NSW	530.0265	704.6030	658.7272	630.7171	
14	Objective function	530.0265	0.3046	3.5351	1.0339e+03	

Table-4 Generation reallocation using MFO algorithm with UPFC at bus 26 on IEEE 30 bus system

S.No	Parameters	OF ₁	OF ₂	OF ₃	OF ₄	
1	Real power generation (MW)	P _{G1}	153.0166	84.6901	56.8950	73.0806
		P _{G2}	43.2944	80.0000	80.0000	63.9987
		P _{G5}	19.6062	50.0000	50.0000	50.0000
		P _{G8}	10.0000	35.0000	35.0000	35.0000
		P _{Gs}	35.0000	25.8898	35.0000	35.0000
		P _{Gw}	30.0000	12.0000	30.0000	30.0000
2	Total real power generation cost (Rs/hr)	579.3646	778.4442	708.0964	680.0312	
3	Active power Loss (MW)	7.5172	4.1799	3.4950	3.6793	
4	Valve point effect(Rs/hr)	605.4616	835.5996	752.5318	737.2706	
5	Voltage deviation (p.u.)	0.3157	0.3022	0.3124	0.3126	
6	Carbon Emission(ton/hr)	0.1268	0.0719	0.0518	0.0527	
7	Q _{UPFC} (p.u)	-0.0579	-0.0556	-0.0571	-0.0571	
8	FPL	49.4666	49.4666	49.4666	49.4666	
9	FPG	579.3646	778.4442	708.0964	680.0312	
10	NSW	529.8980	728.9776	658.6298	630.5646	
11	Objective function	529.8980	0.3022	3.4950	1.0297e+03	

It is observed from Table-2 that the Bus 30 is the most severe bus followed by Bus 26 as indicated by its L-index. UPFC has been placed at bus 30 and bus 26 and the results are presented in Table 3 and Table 4 respectively. L-index is compared with and without UPFC in Fig. 2. It is observed that the L-index of the severe lines have been reduced by the placement of UPFC. Contingency analysis is done for the above system. The most severe contingencies and the lines most effected by the above contingencies are depicted in Table 5, It is observed that line no. 28-27, 9-10 and 27-30 are the most severe contingencies and the buses effected by it are 30 and 19 respectively. The line power flows in the above contingency conditions have been compared in Table-6.

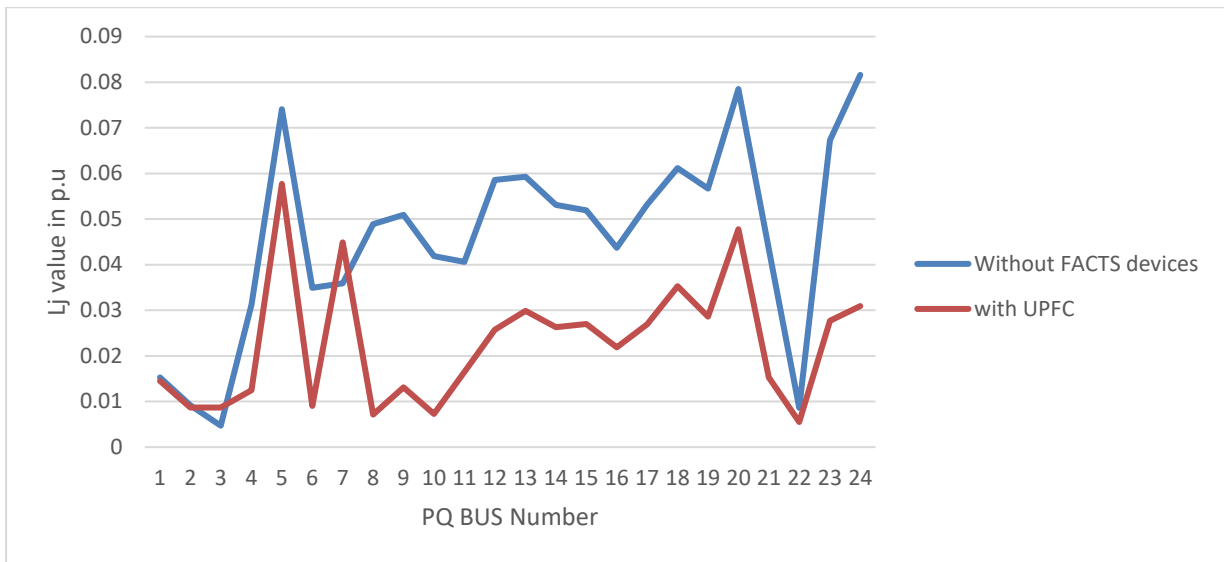


Fig. 4 Comparison of L-index with and without UPFC.

Table-5 Line failures rated as "severe" in descending Lj order

S. No.	Line outage		Severity bus	
	SEB	REB	Lj max Value	BUS no with Lj max
1.	28	27	0.3737	30
2.	9	10	0.1729	19
3.	27	30	0.161	30
4.	27	29	0.1443	30
5.	10	21	0.1282	21
6.	4	12	0.1265	14
7.	25	27	0.1247	26
8.	10	20	0.1217	20
9.	6	28	0.1136	30
10.	19	20	0.1064	19
11.	29	30	0.1053	30
12.	6	8	0.0975	30
13.	1	3	0.0935	30
14.	3	4	0.0928	30
15.	22	24	0.0924	26
16.	2	5	0.0917	30
17.	4	6	0.0908	30
18.	10	22	0.0901	30
19.	2	6	0.0897	30
20.	12	15	0.0864	30
21.	6	10	0.0862	30

S. No.	Line outage		Severity bus	
	SEB	REB	Lj max Value	BUS no with Lj max
22.	23	24	0.0858	30
23.	2	4	0.085	30
24.	18	19	0.0849	30
25.	21	23	0.0848	30
26.	5	7	0.0836	30
27.	8	28	0.0835	30
28.	12	14	0.0833	30
29.	12	16	0.0832	30
30.	15	18	0.083	30
31.	14	15	0.0816	30
32.	15	23	0.0816	30
33.	16	17	0.0812	30
34.	6	7	0.0806	30
35.	6	9	0.0795	30
36.	10	17	0.0794	30
37.	24	25	0.0737	30

Table 6 Contrast of line flows under normal and line outage conditions

SEB	REB	Power flow in line limit (MVA)	Line flows under normal condition	Line flow under Line outage of 28-27
1	2	100	0.3105 - 0.1964i	0.2384 - 0.3564i
1	3	100	0.2308 - 0.2109i	0.2616 - 0.2686i
2	4	100	0.1675 - 0.1614i	0.2260 - 0.1731i
3	4	100	0.2027 - 0.2058i	0.2317 - 0.2568i
2	5	100	0.3651 - 0.2641i	0.3921 - 0.2730i
2	6	100	0.1421 - 0.2719i	0.2000 - 0.3023i
4	6	100	0.1613 - 0.2111i	0.1756 - 0.2118i
5	7	100	-0.0860 - 0.0573i	-0.0603 - 0.0606i
6	7	100	0.3181 - 0.1650i	0.2918 - 0.1604i
6	8	100	-0.2261 - 0.2583i	-0.1384 - 0.2406i
6	9	100	0.0334 + 0.0326i	0.1104 - 0.0406i
6	10	100	0.0874 - 0.0505i	0.1313 - 0.0941i
9	11	100	-0.3500 + 0.3493i	-0.3500 + 0.3467i
9	10	100	0.3834 - 0.3163i	0.4604 - 0.3843i
4	12	100	0.1288 - 0.1514i	0.2000 - 0.2069i
12	13	100	-0.3000 - 0.0135i	-0.3000 - 0.0143i
12	14	100	0.0750 - 0.0155i	0.0864 - 0.0206i

SEB	REB	Power flow in line limit (MVA)	Line flows under normal condition	Line flow under Line outage of 28-27
12	15	100	0.1712 - 0.0325i	0.2116 - 0.0592i
12	16	100	0.0706 - 0.0049i	0.0899 - 0.0163i
14	15	100	0.0122 + 0.0021i	0.0233 - 0.0023i
16	17	100	0.0351 + 0.0142i	0.0541 + 0.0035i
15	18	100	0.0594 - 0.0042i	0.0656 - 0.0065i
18	19	100	0.0269 + 0.0057i	0.0330 + 0.0036i
19	20	100	-0.0681 + 0.0398i	-0.0620 + 0.0378i
10	20	100	0.0914 - 0.0497i	0.0853 - 0.0475i
10	17	100	0.0553 - 0.0733i	0.0364 - 0.0627i
10	21	100	0.1967 - 0.1499i	0.2484 - 0.1919i
10	22	100	0.0695 - 0.0411i	0.1637 - 0.0994i
21	23	100	0.0194 - 0.0330i	0.0694 - 0.0714i
15	23	100	0.0399 + 0.0030i	0.0836 - 0.0228i
22	24	100	0.0689 - 0.0401i	0.1606 - 0.0931i
23	24	100	0.0271 - 0.0136i	0.1200 - 0.0761i
24	25	100	0.0081 + 0.0149i	0.1855 - 0.0880i
25	26	100	0.0355 - 0.0238i	0.0358 - 0.0241i
25	27	100	-0.0275 + 0.0388i	0.1391 - 0.0453i
28	27	100	0.1610 - 0.0870i	-
27	29	100	0.0621 - 0.0171i	0.0630 - 0.0189i
27	30	100	0.0712 - 0.0171i	0.0724 - 0.0193i
29	30	100	0.0371 - 0.0062i	0.0374 - 0.0068i
8	28	100	0.0725 + 0.0423i	0.0214 + 0.0585i
6	28	100	0.0892 - 0.0467i	-0.0212 + 0.0240i

The Optimal power flow for line 28-27 contingency are compared in Table 7. For the above contingencies an UPFC is placed in at bus 30 and the results have been presented in Table 8. It is observed that the loss has been reduced from 7.67 MW to 5.81 MW respectively for line 28-27 contingency.

Table 7 Optimal power flows for various objective functions with line 28-27 contingency and renewable energy sources without UPFC

S.No	Parameter	OF ₁	OF ₂	OF ₃	OF ₄	
1	Real power generation (MW)	P _{G1}	154.7089	50.0000	50.0000	50.0000
		P _{G2}	44.6334	80.0000	65.9036	80.0000
		P _{G5}	20.7118	50.0000	50.0000	50.0000
		P _{G8}	11.9230	60.0000	60.0000	46.0748
		P _{Gs}	35.0000	35.0000	35.0000	35.0000
		P _{Gw}	30.0000	30.0000	30.0000	30.0000
2	Total Active power generation (MW)	296.9771	305	290.9036	291.0748	

S.No	Parameter	OF ₁	OF ₂	OF ₃	OF ₄
3	Total real power generation cost (Rs/hr)	599.5968	792.5050	731.8436	734.9881
4	Active power Loss (MW)	13.5770	21.6000	7.5036	7.6748
5	Valve point effect(Rs/hr)	628.9318	835.3258	778.2820	778.0069
6	Voltage deviation (p.u.)	3.7781	2.5095	2.7190	2.7793
7	Carbon Emission(ton/hr)	0.1302	0.0595	0.0508	0.0524
8	FPL	49.4666	49.4666	49.4666	49.4666
9	FPG	599.5968	792.5050	731.8436	734.9881
10	NSW	550.1302	743.0384	682.3770	685.5215
11	Objective function	550.1302	2.5095	7.5036	1.7309e+03

Table 8 Optimal power flow for various objective functions with contingency at line 28-27 and renewable energy sources with UPFC at Bus 30

S.No	Parameters	OF ₁	OF ₂	OF ₃	OF ₄	
1	Real power generation (MW)	P _{G1}	154.6545	77.3962	59.0389	74.4099
		P _{G2}	43.6828	80.0000	80.0000	64.8082
		P _{G5}	19.7207	50.0000	50.0000	50.0000
		P _{G8}	10.0000	35.0000	35.0000	35.0000
		P _{Gs}	35.0000	35.0000	35.0000	35.0000
		P _{Gw}	30.0000	12.0000	30.0000	30.0000
2	Total Active power generation (MW)	293.0580	289.3962	289.0389	289.2181	
3	Total real power generation cost (Rs/hr)	686.1970	859.4231	813.3162	786.6665	
4	Active power Loss (MW)	9.6580	5.9962	5.6389	5.8181	
5	Valve point effect(Rs/hr)	713.3383	914.5940	859.1175	844.4137	
6	Voltage deviation (p.u.)	0.4490	0.4348	0.4422	0.4427	
7	Carbon Emission(ton/hr)	0.1296	0.0658	0.0531	0.0542	
8	PQsend	0.1190	0.1186	0.1190	0.1190	
9	PQrec	0.0935	0.0938	0.0945	0.0945	
10	Size	V _{cr}	0.0350	0.0350	0.0350	0.0350
		T _{cr}	-87.1236	-87.1236	-87.1236	-87.1236
		V _{vr}	1.0146	1.0145	1.0146	1.0146
		T _{vr}	-24.0483	-22.5569	-20.9503	-21.2679
11	FPL	49.4666	49.4666	49.4666	49.4666	
12	FPG	686.1970	859.4231	813.3162	786.6665	
13	NSW	636.7304	809.9565	763.8496	637.1999	
14	Objective function	636.7303	0.4348	5.6389	1.3633e+03	

The voltage profile of the system with and without FACTS devices has been depicted in Figure 3. The convergence of the multi-objective function without and with UPFC has been compared in Figure 4. The negative social welfare with and without UPFC under various system conditions is shown in Figure 5.

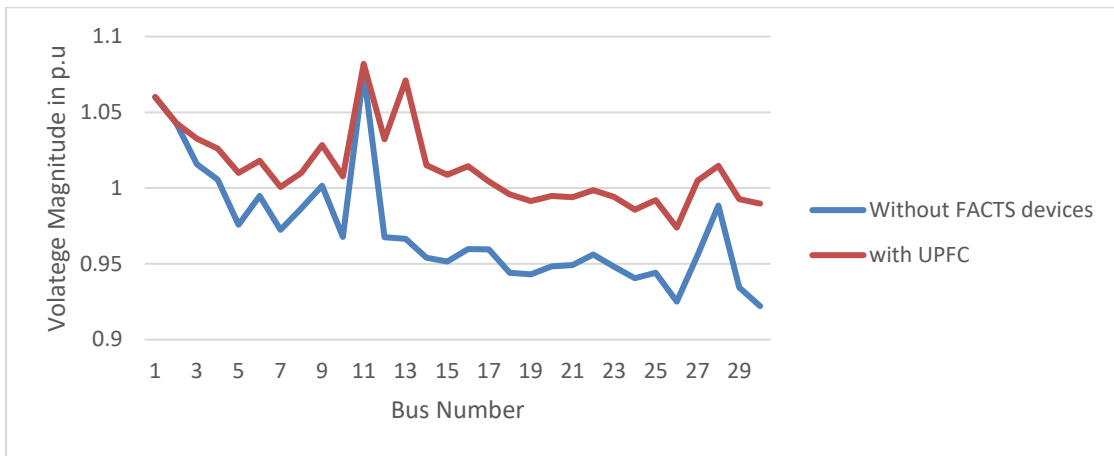


Figure 5 Voltage profile of the multi-objective function.

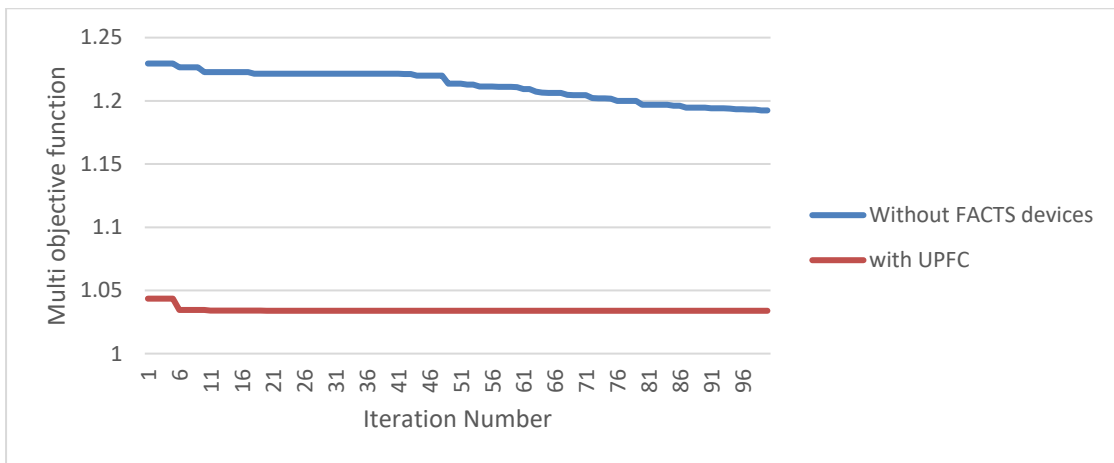


Figure 6 Convergence of the Multi-objective function.

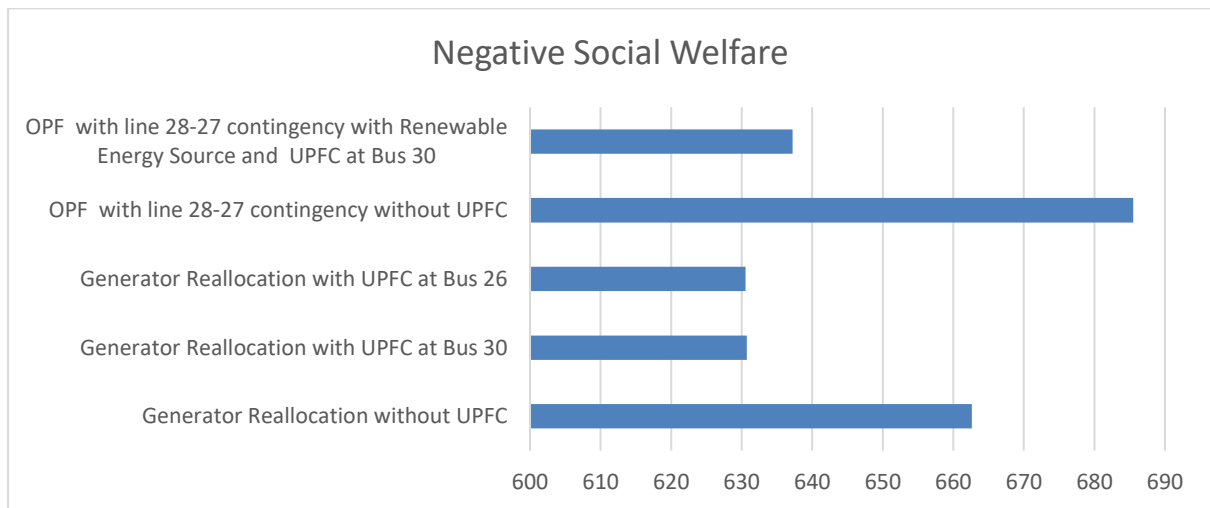


Figure 7 Comparison of Negative Social Welfare with and without UPFC

6. CONCLUSION

A stable power infrastructure is essential to luring in industry and international investment. Consumer participation in the electrical market will grow in significance as the industry undergoes further restructuring. Everyone involved in the electricity system benefits when everyone has access to the price information they need to make informed choices about their energy consumption. Consumers will adjust their energy usage to reflect the value they place on it when

they become exposed to price volatility. The market will be able to make more informed long-term decisions, such as whether and where to invest in expanding the gearbox system, with the support of supplier and consumer input. With the help of FACTS devices, renewable energy sources already a viable alternative to conventional power systems can be made even more stable and reliable. The OPF in the presence of renewable generation effectively improves the power flow capacity of the system. Optimal tuning and placement of UPFC further improves the efficiency of the system. The social welfare is found to improve by 18% after the implementation UPFC in the desired location. Moth Flame optimization is an efficient optimization algorithm which is suited for the multi-objective problem. UPFC being more cost-effective in comparison to the other FACTS devices in the market is a viable option.

7. REFERENCES

- [1] M. O. Lawal, O. Komolafe, and T. O. Ajewole, "Power-flow-tracing-based congestion management in hydro-thermal optimal power flow algorithm," *J. Mod. Power Syst. Clean Energy*, vol. 7, no. 3, pp. 538–548, 2019, doi: 10.1007/s40565-018-0490-5.
- [2] I. Batra and S. Ghosh, "A Novel Approach of Congestion Management in Deregulated Power System Using an Advanced and Intelligently Trained Twin Extremity Chaotic Map Adaptive Particle Swarm Optimization Algorithm," *Arab. J. Sci. Eng.*, vol. 44, no. 8, pp. 6861–6886, 2019, doi: 10.1007/s13369-189018-3675-3.
- [3] K. Teeparthi and D. M. Vinod Kumar, "Multi-objective hybrid PSO-APO algorithm based security constrained optimal power flow with wind and thermal generators," *Eng. Sci. Technol. an Int. J.*, vol. 20, no. 2, pp. 411–426, 2017, doi: 10.1016/j.jestch.2017.03.002.
- [4] Al. Ahmad, S. Ahmad Reza, "Optimal placement and sizing of multi-type FACTS devices in power systems using metaheuristic optimisation techniques: An updated review", *Ain Shams Engineering Journal*, vol. 11, no. 3, pp. 611-628, September 2020
- [5] K. Visakha, D. Thukaram, and L. Jenkins, "Application of UPFC for system security improvement under normal and network contingencies," *Electr. Power Syst. Res.*, vol. 70, no. 1, pp. 46–55, 2004, doi: 10.1016/j.epsr.2003.11.011.
- [6] Nusair, K.; Alasali, F.; Ali, H.; William, H. Optimal placement of FACTS devices and power-flow solutions for a power network system integrated with stochastic renewable energy resources using metaheuristic optimization techniques. *International Journal of Energy Research*, 2021, pg 1-24.
- [7] Subhojit Dawn, Prashant Kumar Tiwari, Arup Kumar Goswami. An approach for long term economic operations of competitive power market by optimal combined scheduling of wind turbines and FACTS controllers. *Energy*, Vol 181, (2019), pg 709-723
- [8] Rui Ma, Xuan Li, Yang Luo, Xia Wu, and Fei Jiang. Multi-objective Dynamic Optimal Power Flow of Wind Integrated Power Systems Considering Demand Response. *CSEE journal of power and energy systems*, VOL. 5, NO. 4, December 2019.
- [9] U. Velayutham, L. Ponnusamy, and G. Venugopal, "Minimization of cost and congestion management using interline power flow controller", *COMPEL - The international journal for computation and mathematics in electrical and electronic engineering*, 2016, vol. 35, no. 5, pp. 1495-1512.
- [10] Suresh Babu Daram; P.S. Venkataramu; M. S. Nagaraj 'Performance index based contingency ranking under line outage condition incorporating IPFC', *International Conference on Electrical, Electronics, and Optimization Techniques (ICEEOT)*, 2016.
- [11] X. S. Yang, "Firefly algorithm, Levy flights and global optimization", *Res. Dev. Intell. Syst.* XXVI, pp. 209–218, 2009.
- [12] M. Akanksha, G. V. Nagesh Kumar, "Line utilisation factor-based optimal allocation of IPFC and sizing using firefly algorithm for congestion management", *IET Generation, Transmission & Distribution*, pp 1-8, 2015.
- [13] G. N. Kumar, M. S. Kalavathi, "Cat Swarm Optimization for optimal placement of multiple UPFC's in voltage stability enhancement under contingency", *Electrical Power and Energy Systems*, vol. 57, pp. 97–104, 2014.
- [14] R. Verma, A. Rathore, "Optimal Placement of Facts Device Considering Voltage Stability and Losses using Teaching Learning based Optimization". *J. Inst. Eng. India Ser. B* 102, pp. 771–776, 2021.
- [15] Adetokun, B. B., Christopher, M. M., 'Application and control of flexible alternating current transmission system devices for voltage stability enhancement of renewable-integrated power grid: A comprehensive review', *Heliyon* 2021 pp 1-7.

- [16] Farid Hamzeh Aghdam, Sina Ghaemi, Amin Safari, Meisam Farrokhifar. Profit-based evaluation of optimal FACTS devices planning for the large consumers and TRANSCO considering uncertainty. *Int Trans Electr Energy Syst.* 2021, pg 1-22, Vol. 31.
- [17] W. A. Oyekanmi, G. Radman, A. A. Babalola, T. O. Ajewole, "Power System Simulation and Contingency Ranking Using Load Bus Voltage Index", IEEE, 2014.
- [18] Sina Ghaemi, Farid Hamzeh Aghdam, Amin Safari, Meisam Farrokhifar, "Stochastic economic analysis of FACTS devices on contingent transmission networks using hybrid biogeography-based optimization" *Electrical Engineering*, 2019 <https://doi.org/10.1007/s00202-019-00825-6>
- [19] Partha P. Biswas, Parul Arora, R. Mallipeddi, P. N. Suganthan, B. K. Panigrahi, Optimal placement and sizing of FACTS devices for optimal power flow in a wind power integrated electrical network, *Neural Computing and Applications*, <https://doi.org/10.1007/s00521-020-05453-x>
- [20] Seyedali Mirjalili, *Moth-Flame Optimization Algorithm: A Novel Nature-inspired Heuristic Paradigm*, *Knowledge-Based Systems* (2015), doi: <http://dx.doi.org/10.1016/j.knosys.2015.07.006>
- [21] Yu Li¹, Xinya Zhu² and Jingsen Liu³, An Improved Moth-Flame Optimization Algorithm for Engineering Problems, *Symmetry* 2020, 12, 1234; doi:10.3390/sym12081234
- [22] Li, G., Li, Q., Yang, X., Ding, R. General Nash bargaining based direct P2P energy trading among prosumers under multiple uncertainties(2022) *International Journal of Electrical Power and Energy Systems*, 143, art. no. 108403, doi=10.1016%2fj.ijepes.2022.108403
- [23] Zhou, Z., Liu, Z., Su, H., Zhang, L. Collaborative strategy of dynamic wireless charging electric vehicles and hybrid power system in microgrid(2022) *International Journal of Electrical Power and Energy Systems*, 143, art. no. 108368, . doi=10.1016%2fj.ijepes.2022.108368
- [24] Baker, K. Emulating AC OPF Solvers with Neural Networks(2022) *IEEE Transactions on Power Systems*, 37 (6), pp. 4950-4953. doi=10.1109%2fTPWRS.2022.3195097
- [25] Lee, J.-O., Kim, Y.-S., Jeon, J.-H. Optimal power flow for bipolar DC microgrids(2022) *International Journal of Electrical Power and Energy Systems*, 142, art. no. 108375, . doi=10.1016%2fj.ijepes.2022.108375
- [26] Sheikhzadehaboli, P., Samimi, A., Ebadi, M., Bayat, M., Pirayesh, A. Frequency control in standalone renewable based-microgrids using steady state load shedding considering droop characteristic(2022) *International Journal of Electrical Power and Energy Systems*, 142, art. no. 108351, .DOI: 10.1016/j.ijepes.2022.108351
- [27] Wang, Q., Lin, S., Gooi, H.B., Yang, Y., Liu, W., Liu, M. Calculation of static voltage stability margin under N-1 contingency based on holomorphic embedding and Pade approximation methods(2022) *International Journal of Electrical Power and Energy Systems*, 142, art. no. 108358, doi=10.1016%2fj.ijepes.2022.108358.
- [28] Majidi, M., Rodriguez-Garcia, L., Mosier, T.M., Parvania, M. Coordinated operation of pumped-storage hydropower with power and water distribution systems(2022) *International Journal of Electrical Power and Energy Systems*, 142, art. no. 108297, . doi=10.1016%2fj.ijepes.2022.108297.
- [29] Chen, Y., Yang, W., Chen, Q., Shi, Z., Yang, L., Wang, X. A quadratic voltage model with modifications for optimal power flow of meshed networks (2022) *International Journal of Electrical Power and Energy Systems*, 142, art. no. 108191, doi=10.1016%2fj.ijepes.2022.108191.
- [30] Zhai, J., Dai, X., Jiang, Y., Xue, Y., Hagenmeyer, V., Jones, C.N., Zhang, X.-P. Distributed Optimal Power Flow for VSC-MTDC Meshed AC/DC Grids Using ALADIN(2022) *IEEE Transactions on Power Systems*, 37 (6), pp. 4861-4873. doi=10.1109%2fTPWRS.2022.3155866.
- [31] Zhang, S., Zhou, M., Liu, Z., Li, G., Zhang, L. Hierarchical Flexible Operation Approach on a VSC-MTDC Interconnected Hybrid Grid with a High Share of Renewable Power(2022) *IEEE Transactions on Power Systems*, 37 (6), pp. 4936-4949. doi=10.1109%2fTPWRS.2022.3155637.
- [32] Zhong, W., Xie, K., Liu, Y., Xie, S., Xie, L. Nash Mechanisms for Market Design Based on Distribution Locational Marginal Prices (2022) *IEEE Transactions on Power Systems*, 37 (6), pp. 4297-4309. doi=10.1109%2fTPWRS.2022.3152517
- [33] Wu, D., Wang, B., Wolter, F.-E., Xie, L. Tri-Sectional Approximation of the Shortest Path to Long-Term Voltage Stability Boundary with Distributed Energy Resources(2022) *IEEE Transactions on Power Systems*, 37 (6), pp. 4720-4731. doi=10.1109%2fTPWRS.2022.3154708.

- [34] Yan, Z., Xu, Y. A Hybrid Data-Driven Method for Fast Solution of Security-Constrained Optimal Power Flow (2022) IEEE Transactions on Power Systems, 37 (6), pp. 4365-4374. doi=10.1109%2fTPWRS.2022.3150023.
- [35] Ryu, M., Nagarajan, H., Bent, R. Mitigating the Impacts of Uncertain Geomagnetic Disturbances on Electric Grids: A Distributionally Robust Optimization Approach (2022) IEEE Transactions on Power Systems, 37 (6), pp. 4258-4269. doi=10.1109%2fTPWRS.2022.3147104.
- [36] Brust, J.J., Anitescu, M. Convergence Analysis of Fixed Point Chance Constrained Optimal Power Flow Problems (2022) IEEE Transactions on Power Systems, 37 (6), pp. 4191-4201. doi=10.1109%2fTPWRS.2022.3146873.
- [37] Subramanyam, A., Roth, J., Lam, A., Anitescu, M. Failure Probability Constrained AC Optimal Power Flow (2022) IEEE Transactions on Power Systems, 37 (6), pp. 4683-4695. doi=10.1109%2fTPWRS.2022.3146377.
- [38] Chopra, S., Vanaprasad, G.M., Tinajero, G.D.A., Bazmohammadi, N., Vasquez, J.C., Guerrero, J.M. Power-flow-based energy management of hierarchically controlled islanded AC microgrids (2022) International Journal of Electrical Power and Energy Systems, 141, art. no. 108140, doi=10.1016%2fj.ijepes.2022.108140.
- [39] Xu, T., Ding, T., Han, O., Huang, Y., He, Y. Counterpart and Correction for Strong Duality of Second-Order Conic Program in Radial Networks (2022) IEEE Transactions on Power Systems, 37 (5), pp. 4117-4120. doi=10.1109%2fTPWRS.2022.3173539.
- [40] Mohammadi, S., Hesamzadeh, M.R., Bunn, D.W. Distribution Locational Marginal Pricing (DLMP) for Unbalanced Three-Phase Networks (2022) IEEE Transactions on Power Systems, 37 (5), pp. 3443-3457. doi=10.1109%2fTPWRS.2021.3138798.
- [41] Liu, J., Yang, Z., Zhao, J., Yu, J., Tan, B., Li, W. Explicit Data-Driven Small-Signal Stability Constrained Optimal Power Flow (2022) IEEE Transactions on Power Systems, 37 (5), pp. 3726-3737. doi=10.1109%2fTPWRS.2021.3135657.
- [42] Agarwal, A., Pileggi, L. Large Scale Multi-Period Optimal Power Flow With Energy Storage Systems Using Differential Dynamic Programming (2022) IEEE Transactions on Power Systems, 37 (3), pp. 1750-1759. doi=10.1109%2fTPWRS.2021.3115636.
- [43] Heidarifar, M., Andrianesis, P., Ruiz, P., Caramanis, M.C., Paschalidis, I.C. An optimal transmission line switching and bus splitting heuristic incorporating AC and N-1 contingency constraints (2021) International Journal of Electrical Power and Energy Systems, 133, art. no. 107278, . doi=10.1016%2fj.ijepes.2021.107278.
- [44] Zhao W, Wang L, Zhang Z. Artificial ecosystem-based optimization: a novel nature-inspired meta-heuristic algorithm. *Neural Comput Appl*. 2020; 32:9383-9425.
- [45] Ugranli F, Karatepe E. Coordinated TCSC allocation and network reinforcements planning with wind power. *IEEE Trans Sustainable Energy*. 2017; 8:1694-1705.
- [46] Ziaee O, Choobineh F. Optimal location-allocation of TCSC devices on a transmission network. *IEEE Trans Power Syst*. 2017; 32:94-102.
- [47] Sahraei-Ardakani M, Hedman W. A fast Ip approach for enhanced utilization of variable impedance-based facts devices. *IEEE Trans Power Syst*. 2016;31(3):2204-2213. <https://doi.org/10.1109/PESGM.2016.7741200>.
- [48] Biswas P, Suganthan N, Mallipeddi R, Amaratunga A. Optimal reactive power dispatch with uncertainties in load demand and renewable energy sources adopting scenario-based approach. *Appl. Soft Comput*. 2019; 75:616-632.

DOI: <https://doi.org/10.15379/ijmst.v10i1.2639>

This is an open access article licensed under the terms of the Creative Commons Attribution Non-Commercial License (<http://creativecommons.org/licenses/by-nc/3.0/>), which permits unrestricted, non-commercial use, distribution and reproduction in any medium, provided the work is properly cited.